Korean J Physiol Pharmacol
Vol 7: 47−52, February, 2003

Effects of Noradrenaline on the Membrane Potential of Prostatic Neuroendocrine Cells of Rat

Jun Hee Kim, Sun Young Shin, Dae-Yong Uhm, and Sung Joon Kim

Department of Physiology, Sungkyunkwan University School of Medicine, Suwon 440-746, Korea

The prostate gland contains numerous neuroendocrine cells that are believed to influence the function of the prostate gland. Our recent study demonstrated the expression of both α1- and α2-ARs, signaling the release of stored Ca^{2+} and the inhibition of N-type Ca^{2+} channels, respectively, in rat prostate neuroendocrine cells (RPNECs). In this study, the effects of NA on the resting membrane potential (RMP) of RPNECs were investigated using a whole-cell patch clamp method. Fresh RPNECs were dissociated from the ventral lobe of rat prostate and identified from its characteristic shape; round or oval shape with dark cytoplasm. Under zero-current clamp conditions with KCl pipette solution, the resting membrane potential (RMP) of RPNECs was between -35 mV and -85 mV. In those RPNECs with relatively hyperpolarized RMP (<-60 mV), the application of noradrenaline (NA, 1μM) depolarized the membrane to around -40 mV. In contrast, the RPNECs with relatively depolarized RMP (>-45 mV) showed a transient hyperpolarization and subsequent fluctuation at around -40 mV on application of NA. Under voltage clamp conditions (holding voltage, -40 mV) with CsCl pipette solution, NA evoked a slight inward current (<-20 pA). NA induced a sharp increase of cytosolic Ca^{2+} concentration ($[Ca^{2+}]_c$), measured by the fura-2 fluorescence, and the voltage clamp study showed the presence of charybdotoxin-sensitive Ca^{2+}-activated K^+ currents. In summary, adrenergic stimulation induced either depolarization or hyperpolarization of RPNECs, depending on the initial level of RMP. The inward current evoked by NA and the Ca^{2+}-activated K^+ current might partly explain the depolarization and hyperpolarization, respectively.

Key Words: Prostate, Neuroendocrine cell, Noradrenaline, Membrane potential, Patch clamp

INTRODUCTION

The human prostate is a major accessory gland of male reproductive system and the site where the largest number of urological problems, including benign prostate hyperplasia (BPH), can arise. In spite of the clinical importance, knowledge about the normal physiology of the prostate gland is very poor. The prostate gland consists of a complex ductal system lined with exocrine epithelial cells, neuroendocrine (NE) cells and basal stem cells embedded in a stromal matrix (McNeal, 1988). Prostate NE cells with paracrine/autocrine properties may regulate the growth, as well as the function, of surrounding cells and the stromal matrix (di Sant'Agnese et al, 1987; Cohen et al, 1993). The density of chromogranin-A positive neuroendocrine cells is reported to be higher in the neoplastic region of prostate hyperplasia than in the normal prostate (Guate et al, 1997; Bonkhoff, 1998). Focal neuroendocrine differentiation occurs in prostatic adenocarcinomas and those tumors with extensive and multifocal neuroendocrine differentiation tend to be more aggressive and resistant to hormonal therapy, providing a prognostic marker of the prostate cancer (di Sant'Agnese et al, 1987; Guate et al, 1997; Bonkhoff, 1998). Based on immunohistochemical studies, NE cells of the prostate are believed to secrete a variety of neurosecretory products such as serotonin, histamine, calcitonin and parathyroid hormone-related peptides (Vittoria et al, 1990; Polge et al, 1998).

In our recent studies, single prostate cells were isolated by an enzymatic digestion of the ventral lobe of rat prostate and were utilized for the patch clamp study. Among the cells isolated, columnar cells with a pale cytoplasm, and round or oval-shaped cells with a dark cytoplasm (round-cells) were the most abundant (Kim et al, 2002; Kim et al, 2003a, 2003b). These two groups of cells were distinguishable not only by their morphology, but also by their electrophysiological properties. In columnar cells of the prostate, step-like depolarization of the membrane activated a time-independent outward current that was markedly augmented by muscarinic or purinergic stimulation (Kim et al, 2002a). Also, we found the Ca^{2+}-activated Cl^- current that had time-dependent slow activation kinetics (Kim et al, 2003a). These Ca^{2+}-activated ion channels might explain the exocrine secretion of electrolyte and fluid in prostate glands. In contrast, the round-cells

Corresponding to: Sung Joon Kim, Department of Physiology, Sungkyunkwan University School of Medicine, Suwon 440-746, Korea. (Tel) +82-31-299-6104, (Fax) +82-31-299-6129, (E-mail) sjoonkim@med.skku.ac.kr

ABBREVIATIONS: RPNEC, rat prostate neuroendocrine cell; NA, noradrenaline; RMP, resting membrane potential; APs, Action potentials.

displayed transient-type outward currents, high voltage-activated Ca^{2+} current (HVA-I_{Ca}) and TTX-resistant Na^{+} current (Kim et al, 2003b). In addition to their electrically excitable properties, the immunofluorescence study demonstrated the presence of chromogranin-A in round-cells, a representative marker of neuroendocrine cells (Kim et al, 2003b). All these results commonly indicate that the round-cells dissociated from the prostate are putative rat prostate neuroendocrine cells (RPNECs).

The physiological function of prostate is under the control of autonomic nervous system as well as the hormonal state (McVerry et al, 1999). The secretion of prostatic fluid, for example, is positively regulated by acetylcholine (ACh) via muscarinic receptors in the secretory epithelial cells (Wang et al, 1991). On the other hand, α-adrenergic stimulation induces the smooth muscle contraction that would help the secreted fluid to be expelled from the lumen of gland (Wang et al, 1991; Chapple, 2001). Compared with the above studies on the influence of autonomic neurons to physiological functions of prostate epithelial- and smooth muscle cells, the regulation of neuroendocrine cells have yet rarely been investigated. When the aforementioned putative RPNECs were applied to the fura-2 fluorescence measurement and the whole-cell patch clamp technique, it was clearly demonstrated that α1- and α2-adrenergic stimulations were coupled with stored Ca^{2+} release and inhibition of HVA-I_{Ca}, respectively (Kim et al, 2003c).

The membrane potential of RPNECs would play important roles in determining the excitability; i.e. generation of action potentials and Ca^{2+} influx via voltage-operated Ca^{2+} channels. Considering the importance of noradrenaline (NA) in the regulation of prostatic neuroendocrine cells, we investigated the effects of NA on the membrane potential of RPNECs. Our results demonstrated that NA could induce both depolarization and hyperpolarization of RPNECs, depending on their initial membrane potential.

METHODS

Cell isolation

All procedures on experimental animals were performed in accordance with the guidelines of the Institutional Animal Care and Use Committee (IACUC) of Sungkyunkwan University. Sprage-Dawley rats (male, 350~400 g, n=55) were killed by 100% CO_2 inhalation, and the ventral lobe of the prostate gland was removed immediately thereafter. The fibrous capsule was removed, and the tissue was cut with scissors into small pieces (1~2 mm^3) in a phosphate-buffered Ca^{2+}-free Tyrode's solution. The tissue was digested for 25 min at 37°C in Ca^{2+}-free Tyrode's solution containing collagenase (2 mg/ml, Wako, Japan), trypsin inhibitor (1 mg/ml, Sigma, St. Louis, USA), bovine serum albumin (3 mg/ml, Sigma) and dithiothreitol (1 mg/ml, Sigma). Following digestion and subsequent removal of supernatant, tissue segments were transferred to fresh Tyrode's solution and agitated gently using a fire-polished wide bore (1~2 mm) Pasteur pipette. Cells were isolated daily, and then stored in fresh solution at 4°C for up to 6 h. Dispersed cells were transferred to an experiment chamber and examined by an inverted microscope (IX-70, Olympus, Japan).

Fresh single cells were isolated daily and used for the subsequent electrophysiological study. For hematoxylin-eosin (H-E) staining, cells were cytospun onto silane-coated slides (Muto Pure Chemical, Japan), air-dried, and prepared for the standard staining procedure (Fig. 1). Round or oval shape cells with relatively dark cytoplasm were regarded as RPNECs. The putative RPNECs were easily distinguishable from the elongated columnar epithelial cells and used for the subsequent study.

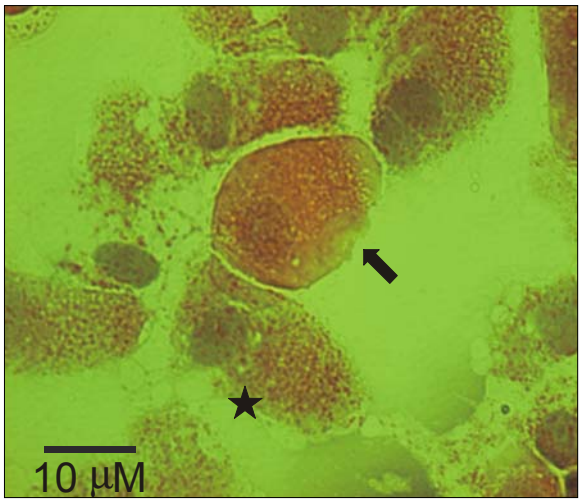

Fig. 1. Morphology of single prostate cells. H & E staining. Note the two different types of cells, namely the columnar (asterisk) and round (arrow) cells. The round cell with darker cytoplasm was regarded here to be neuroendocrine cells. Due to the cytospinning procedure, initially isolated cells became flattened and clumped.

Intracellular Ca^{2+} measurement

Isolated single cells were loaded with acetoxymethyl ester form of fura-2 (2μM) in the Ringer's solution for 20 min at room temperature and then washed out with fresh solution. The recording of $[Ca^{2+}]_c$ was performed with a microfluorimetric system consisting of an inverted fluorescence microscope (Olympus IX-70, Japan) with a dry-type fluorescence objective lens (×40, NA 0.85), a photomultiplier tube (type R 1527, Hamamatsu, Japan) and Deltascan illuminator (Photon Technology International Inc, USA). Light was provided by a 75-W xenon lamp (Ushino, Japan), a chopper wheel alternated the light path to monochromators (340 and 380 nm) with a frequency of 5 Hz, and intensity of emitted light at 510 nm was measured. As a measure of $[Ca^{2+}]_c$ the fluorescence emission ratio at 340 nm/380 nm excitation ($F_{340/380}$) is presented.

Patch-clamp methods

Isolated cells were transferred to a bath situated on the stage of an inverted microscope (IX-70, Olympus). The bath (approximately 0.3 ml) was superfused at 10 ml/min, and voltage clamp experiments were performed at room temperature (22~25°C). Patch pipettes (with a free-tip resistance 2.5~3 MOhm) were connected to the head stage of a patch clamp amplifier (Axopath 1-D, Axon Instruments, Foster City, USA). Liquid junction potentials were corrected with an offset circuit before each experiment. For

the perforated whole-cell patch clamp, a stock solution of nystatin in dimethylsulfoxide (15 mg/ml) was added to the pipette solution, yielding a final concentration of 0.15 mg/ml. A steady-state perforation was usually achieved within ten minutes after making a giga-seal. pCLAMP software v.7.0 and Digidata-1200A (both from Axon Instruments) were used for the acquisition of data and the application of command pulses. The voltage and current data were low-pass filtered (5 kHz) and displayed on a computer monitor. Current traces were stored in a Pentium-grade computer and analyzed using Origin v. 6.1 (Microcal Software Inc, Northampton, USA).

Solution and drugs

All the experiments were performed in Tyrode's solution containing 145 mM NaCl, 1.6 mM K_2HPO_4, 0.4 mM KH_2PO_4, 1 mM $MgCl_2$ and 5 mM *D*-glucose at pH 7.4 titrated with NaOH. $CaCl_2$ was omitted from the enzymatic isolation of single prostate cells. The KCl pipette solution for recording membrane potential and K^+ current in nystatin-perforated conditions contained 130 mM KCl, 1 mM $MgCl_2$, 0.5 mM EGTA, 5 mM *D*-Glucose and 10 mM HEPES at pH 7.2, titrated with KOH. The CsCl pipette solution for a conventional whole-cell mode experiments contained 130 mM CsCl, 1 mM $MgCl_2$, 10 mM EGTA, 5 mM *D*-Glucose and 10 mM HEPES at pH 7.2, titrated with CsOH. All the drugs and chemicals used were bought from Sigma (St Louis, USA).

RESULTS

Single cells isolated from the rat ventral prostate

After the isolation of single cells, at least three cell types could be discriminated; 1) columnar cells with pale cytoplasm, 2) round or oval-shaped cells with a dark cytoplasm and 3) thin spindle-shaped cells that were most likely smooth muscle cells or fibroblasts. Fig. 1 shows an example of H-E stained prostate cells after the procedure of single cell isolation. Although the cells tended to flatten during the cytospin and fixation procedures, distinct cell morphologies could still be discriminated. The columnar cells, indicated by an asterisk, are exocrine secretory epithelial cells (Lee & Holland, 1987; Kim et al, 2002). The cell marked by an arrow had a relatively round shape with dark cytoplasm, and these round cells displayed immunoreactivity to anti-chromogranin A antibody, a representative marker of neuroendocrine cells in various organs (data not shown, but see Kim et al, 2003b). From the morphological study, the round cells isolated by the enzymatic digestion were tentatively regarded as putative RPNE cells and were used in the following study.

Membrane potential of RPNECs

After achieving a steady-state nystatin-perforation with a KCl pipette solution, the round cells had hyperpolarized resting membrane potential values (RMPs), ranging from -85 mV to -35 mV, under zero-current clamp conditions. Fig. 2 shows original traces of the membrane potential obtained from different RPNECs. Usually, the RMP of RPNECs were more negative than -60 mV and calm (Type I cells, Fig. 2A) and, in other cases, RMPs were relatively depolarized ($\geq$-45 mV, Type II cells) and showed a spontaneous generation of action potentials (APs, Fig. 2B). The distribution of RMPs measured in putative RPNECs has been analyzed in our previous study, where about 70% of tested cells showed relatively hyperpolarized initial RMP ($<$-60 mV, 70 out of 96 cells, Kim et al, 2003b).

A slow pacemaker-like depolarization preceded a rapid upstroke of AP (see the expanded chart trace in Fig. 2B). The putative RPNECs with initially hyperpolarized RMPs were able to generate APs, once they were depolarized by experimental maneuvers such as K^+ channel blocker or depolarizing current injection. Fig. 2C present a representative effect of Ba^{2+} (0.2 mM), a K^+ channel blocker, on the membrane potential of RPNEC. In another case where spontaneous APs were already observed, the application of K^+ channel blocker (e.g. TEA^+) increased the amplitude of APs (Fig. 2D).

Effects of NA on the membrane potential of RPNECs

In putative RPNECs, the changes in membrane potential was different depending on the membrane voltages of RMP. In Type I cells with relatively hyperpolarized RMP, the

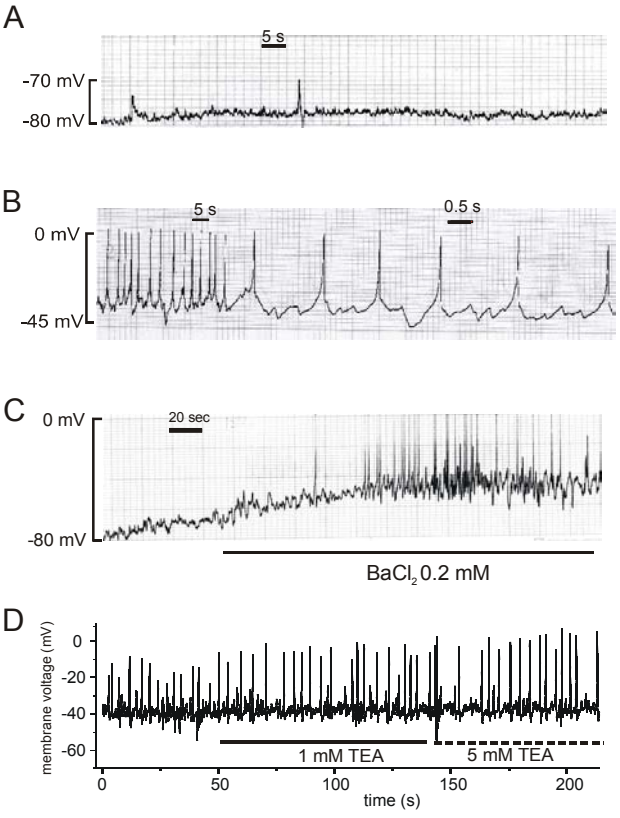

Fig. 2. Classification of RPNECs based on RMP. (A) A representative example of a RPNEC with initially hyperpolarized RMP (-80 mV). A brief fluctuation of membrane potential was observed, but did not lead to action potential. (B) A representative example of a RPNEC with initially depolarized RMP (-40 mV) superimposed with spontaneous APs. Note the different time scales. (C) In a hyperpolarized RPNEC, $BaCl_2$ (0.2 mM) induced membrane depolarization and subsequent burst of action potentials. (D) The amplitude of spontaneous APs was augmented by treatment with TEA.

application of NA induced a depolarization that was reversed by a washout with control solution (Fig. 3). In a single case, a generation of AP was superimposed on the NA-induced depolarization (Fig. 3A, upper trace), demonstrating the increase of excitability. However, in most other cases, the NA-induced depolarization failed to generate APs (see *Discussion*). The NA-induced depolarization was persistent in the presence of NA, but showed more frequent fluctuation of the membrane voltage. Fig. 3B summarizes the change of RMPs recorded in eight RPNECs.

In contrast to the above responses, Type II cells with initially depolarized RMPs showed a transient hyperpolarization upon the application of NA (Fig. 4). Interestingly, the NA-induced fluctuation of membrane voltage in the steady-state was similar to the one observed in RPNECs with hyperpolarized initial RMP. The fluctuation of membrane voltage was markedly reduced by the treatment with Ba^{2+} (0.2 mM), a K^+ channel blocker, while the initial transient hyperpolarization was persistent (Fig. 4A, lower trace). Such hyperpolarizing responses were observed in four cases out of 12 cells tested and summarized in Fig. 4B.

Mechanism of the NA-induced changes in membrane potential of RPNECs

To investigate the underlying changes in the membrane conductance induced by NA, the membrane voltage was clamped at -40 mV and ramp-like hyperpolarizing pulses (from +60 to -100 mV, 0.1 V/s) were applied at every 5 s. To prevent the activation of K^+ channel currents, CsCl pipette solution containing high concentration of EGTA (10 mM) was used for the conventional mode of whole-cell patch clamp. To minimize the interference from voltage-operated Ca^{2+} currents, the membrane voltage was initially depolarized at +60 mV for 500 ms, and then hyperpolarized to obtain a brief current to voltage relation (I-V curves). An original trace of membrane currents showed a very slight downward deflection of holding current by the application of NA (1μM), suggesting an activation of cationic conductance (Fig. 5A). However, the change in membrane conductance was so small that the I/V curves obtained in the control and NA conditions did not clearly reveal a discernable increase in cationic conductance by NA (Fig. 5B, n=5).

We have recently reported that RPNECs express Ca^{2+}-

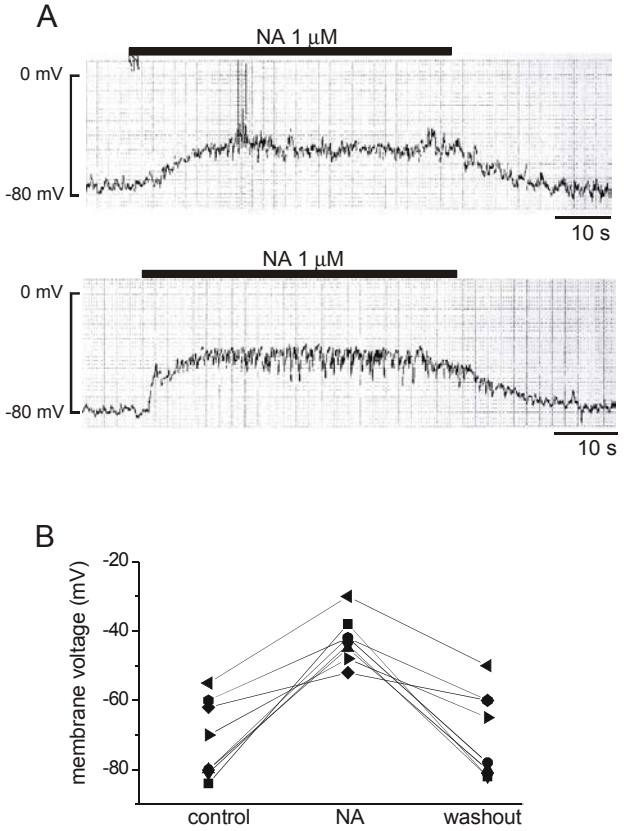

Fig. 3. Membrane depolarization induced by NA treatment. (A) Representative traces of membrane voltage recorded under the nystatin-perforated mode of zero-current clamp. The bath application of NA (1μM) slowly depolarized the membrane to -40 mV, which was superimposed by hyperpolarizing fluctuations of membrane voltage. Note the spontaneous generation of action potentials in the upper trace. (B) Summary of the membrane voltages measured in eight RPNECs. Different symbols indicate different cells.

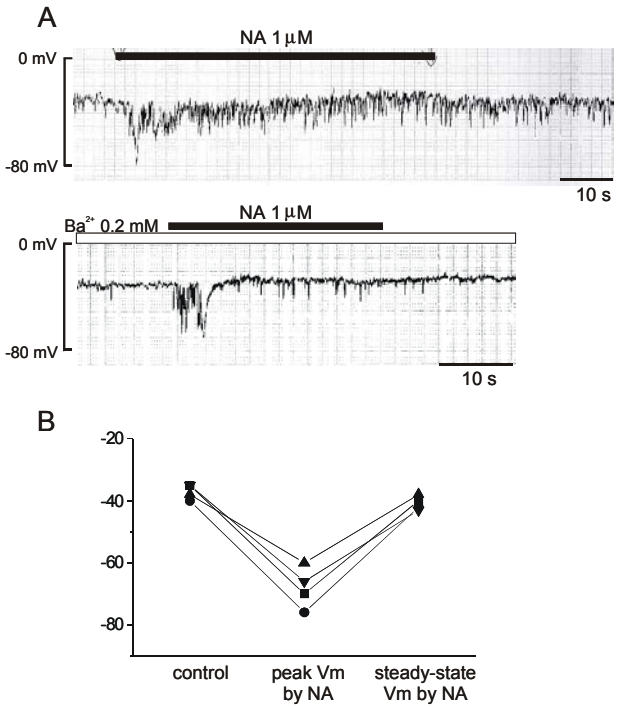

Fig. 4. Transient membrane hperpolarization induced by NA treatment. (A) Representative original traces of membrane voltage recorded under the nystatin-perforated mode of zero-current clamp. The membrane voltage was hyperpolarized by the bath application of NA (1μM) and subsequent hyperpolarizing fluctuations were prominent. The pretreatment with $BaCl_2$ (0.2 mM) markedly abolished the hyperpolarizing fluctuations, while the transient hyperpolarization by NA was still observed (lower trace). (B) Summary of the membrane voltages measured in four RPNECs with initially depolarized membrane voltages. Different symbols indicate different cells.

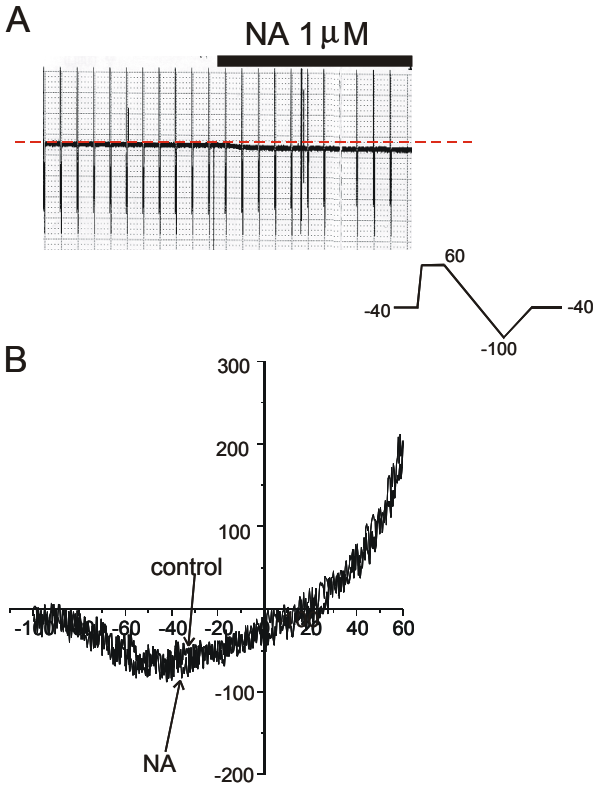

Fig. 5. The inward current induced in RPNEC by NA. (A) A representative original trace of membrane current recorded from the cell held at -40 mV. A CsCl pipette solution was used for the conventional whole-cell patch clamp. The horizontal dotted line was laid to indicate the level of holding current at the initial control condition. Hyperpolarizing ramp-like pulses (see the protocol shown in the *inset*) were applied at every 5 s, and the I/V curves obtained were plotted in (B).

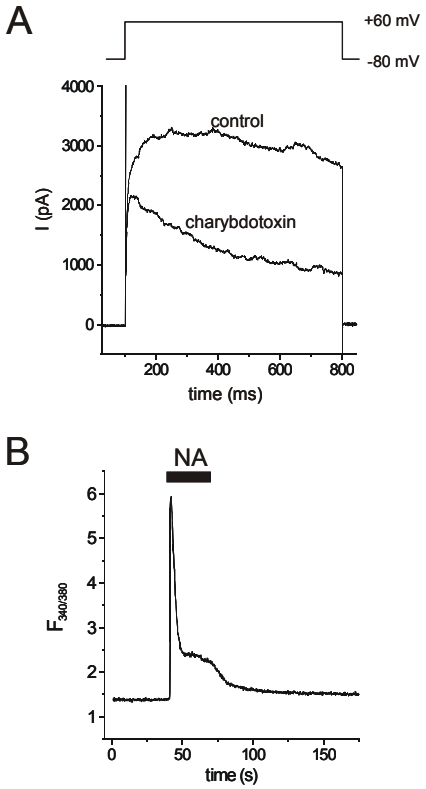

Fig. 6. NA-induced increase of $[Ca^{2+}]_c$ and Ca^{2+}-activated K^+ current in RPNECs. (A) Outward K^+ current evoked by a step-like depolarization from -80 mV to +60 mV. Nystatin-perforated whole-cell clamp was done with KCl pipette solution. The amplitude of outward current was markedly decreased by the bath application of charybdotoxin (100 nM), a specific blocker of Ca^{2+}-activated K^+ channels (B).

activated K^+ channels that are blocked by various blockers (Kim et al, 2003a). In the present experiment, KCl pipette solution was used and nystatin-perforated mode of voltage clamp was adopted to apply a depolarizing step pulse. Fig. 6A demonstrates a representative response of outward potassium current to charybdotoxin (200 nM), a blocker of maxi-K or SK4 type of Ca^{2+}-activated K^+ channels. The steady-state outward current was more selectively suppressed by charybdotoxin, whereas the initial transient component was relatively resistant.

When cells are equipped with Ca^{2+}-activated K^+ channels, an increase of cytosolic calcium activity ($[Ca^{2+}]_c$) might be able to evoke the membrane hyperpolarization of RPNEC. As depicted in Fig. 6B, the application of NA in fact induced a sharp increase of $[Ca^{2+}]_c$. For this experiment, cells were loaded with fura-2, and the fluorescence ratio ($F_{340/380}$) was monitored to reveal the changes in $[Ca^{2+}]_c$. In those cells identified as putative RPNECs by their morphology, an application of NA unexceptionally increased $F_{340/380}$ which was composed of an initial transient peak and plateau (n=20).

DISCUSSION

In this study, we investigated the effects of NA on the membrane potential of putative neuroendocrine cells dissociated from the ventral lobe of rat prostate. The round-shaped cells of rat prostate (putative RPNECs) showed either hyperpolarized (Type I) or depolarized RMPs (Type II) after achieving a steady-state nystatin-perforation with a KCl pipette solution. According to our recent study, the mean of RMPs recorded in putative RPNECs was -70 mV (Kim et al, 2003b). The spontaneous generation of APs could be observed in those cells with relatively depolarized initial RMPs ($\geq$-50 mV) and also under the application of K^+ channel blockers. The presence of APs unequivocally indicates that the cells investigated here are electrically excitable.

Role of adrenoceptors in the prostate neuroendocrine cells

Besides their actions on secretory epithelial cells and smooth muscle cells, the regulation of paracrine secretion from the prostatic neuroendocrine cells by autonomic nerves is a crucial step in physiological functioning of the

prostate gland. In human prostate tissue, for example, the stimulation of adrenoceptors (ARs) with NA induces the release of histamine that is believed to originate from PNECs (Polge et al, 1998). In the above study, the effect of NA was blocked by α1-AR antagonist, whereas the addition of α2-AR antagonist enhanced the release of histamine. Moreover, both basal- and NA-induced release of histamine were suppressed by clonidin, an α2-AR agonist (Polge et al, 1998). We recently attempted to explain such a bi-directional effects of NA in prostate neuroendocrine cells, which demonstrates the increase of $[Ca^{2+}]_c$ by α1-ARs and the inhibition of HVA-I_{Ca} by α2-ARs (Kim et al, 2003b). The strong inhibition of HVA-I_{Ca} by α2-adrenergic stimulation might explain the rare generation of APs during the NA-induced depolarization, observed in this study (Fig. 2). The increase of $[Ca^{2+}]_c$ by NA was also shown in this study, and its transient nature might be associated with the phasic hyperpolarization induced by NA via activation of K_{Ca} channels (see below).

The mechanism of NA-induced changes in membrane potential

In this study, NA consistently induced a sustained depolarization of Type I RPNECs. Interesting, it appeared that the NA-induced depolarization did not surpass a kind of limit at around -40 mV, as if it was equilibrated with an opposite hyperpolarizing influence. In this respect, an intriguing finding of present study was that Type II RPNECs showed only a transient hyperpolarization and subsequent fluctuation of membrane potential at around -40 mV. Therefore, it was very likely that the activation of K^+ conductance from above -40 mV (e.g. Kv channels or Maxi-K channels) might put a brake on the NA-induced depolarizing tendency. In this respect, the initial hyperpolarizing response of Type II cells to NA (Fig. 4) might be explained by a transient activation of Ca^{2+}-activated K^+ channels (K_{Ca}) tightly associated with the increase of $[Ca^{2+}]_c$ (Fig. 6). Due to their voltage-dependence, charybdotoxin-sensitive K_{Ca} may probably exert their hyperpolarizing effect more effectively in Type II cells than in Type I cells.

The mechanism of NA-induced depolarization is, however, not yet clear. We were able to identify a slight inward current at a negative holding voltage, suggesting an activation of nonselective cationic channels. Only a minute activation of inward current might be able to depolarize the RPNEC at hyperpolarized state, where the input resistance would be high. However, the I/V curves obtained by ramp pulses did not allow us to analyze such a slight change of membrane conductance (Fig. 5). In the strong Ca^{2+} buffering condition of the present study (10 mM EGTA), however, there was a possibility that Ca^{2+}-dependent cationic channels, if any, could not have been activated. Different mode of patch clamp experiment (e.g. nystatin-perforated clamp) might be helpful to reveal the NA-induced membrane conductance.

Another possible mechanism of membrane depolarization is that NA might reduce the background K^+ conductance or inwardly-rectifying K^+ currents, which was not examined here. Further investigation was desired to elucidate precise mechanisms of NA-induced depolarization.

In summary, adrenergic stimulation induces either depolarization or hyperpolarization of RPNECs, depending on the initial level of RMP. The inward current evoked by NA and the Ca^{2+}-activated K^+ current may partly explain the depolarization and hyperpolarization, respectively.

ACKNOWLEDGEMENTS

This study was supported by a grant of the Korea Health 21 R&D Project, Ministry of Health & Welfare, Republic of Korea (01-PJ1-PG3-21400-0019).

REFERENCES

Bonkhoff H. Neuroendocrine cells in benign and malignant prostate tissue: morphogenesis, proliferation, and androgen receptor status. Prostate 8(suppl): 18-22, 1998

Chapple CR. Alpha adrenoceptor antagonists in the year 2000: is there anything new? *Curr Opin Urology* 11: 9-16, 2001

Cohen RJ, Glezerson G, Taylor LF, Grundle HA, Naude JH. The neuroendocrine cell population of the human prostate gland *J Urol* 150: 365-368, 1993

di Sant'Agnese PA, Davis NS, Chen M, de Mesy Jensen KL. Age-related changes in the neuroendocrine (endocrine-paracrine) cell population and the serotonin content of the guinea pig prostate. *Lab Invest* 57: 729-736, 1987

Guate JL, Escaf S, Menendez CL, Valle M, Vega JA. Neuroendocrine cells in benign prostatic hyperplasia and prostatic carcinoma: effect of hormonal treatment. *Urol Int* 59: 149-153, 1997

Kim JH, Hong EK, Choi HS, Oh SJ, Kim KM, Uhm DY, Kim SJ. K^+ channel currents in rat ventral prostate epithelial cells. *Prostate* 51: 201-210, 2002

Kim SJ, Shin SY, Lee JE, Kim JH, Uhm DY. Ca^{2+}-activated Cl^- channel currents in rat ventral prostate epithelial cells. *Prostate* in press, 2003a

Kim JH, Shin SY, Yun SS, Kim TJ, Hong EK, Chung YS, Oh SJ, Kim KM, Uhm D-Y, Kim SJ. Voltage-dependent ion channel currents in neuroendocrine cells of the rat prostate. *Pflgers Arch*, in press, 2003b

Kim JH, Shin SY, Nam JH, Hong EK, Chung Y-S, Jeong JY, Kang J, Uhm DY, Kim SJ. Adrenergic regulation of the intracellular $[Ca^{2+}]$ and voltage-operated Ca^{2+} channel currents in the rat prostate neuroendocrine cells. *Prostate*, under revision, 2003c.

Lee C, Holland JM. Anatomy, histology, and ultra-structure (correlation with function), Prostate, Rat. In: Jones TC, Mohr U, Hunt RD ed, *Genital System (Monographs on Pathology of Laboratory Animals.* Springer-Verlag, Berlin, p 239-251, 1987

McNeal JE. Normal histology of the prostate. *Am J Surg Pathol* 12: 619-633, 1988

McVary KT, McKenna KE, Lee C. Prostate innervation. *Prostate* 8(suppl): 2-13, 1999

Polge A, Gaspard C, Mottet N, Guitton C, Boyer JC, Choquet A, Combettes S, Bancel E, Costa P, Bali JP. Neurohormonal stimulation of histamine release from neuroendocrine cells of the human adenomatous prostate. *Prostate* 34: 1-9, 1998

Vittoria A, La Mura E, Cocca T, Cecio A. Serotonin-, somatostatin- and chromogranin A-containing cells of the urethro-prostatic complex in the sheep. An immunocytochemical and immunofluorescent study. *J Anat* 171: 169-178, 1990

Wang JM, McKenna KE, Lee C. Determination of prostatic secretion in rats. *Prostate* 18: 289-301, 1991